European Review for Medical and Pharmacological Sciences 2023; 27: 3631-3644

Unravelling the antibacterial potential of biosynthesized selenium nanoparticles against *Salmonella Typhimurium* food pathogen: *in vitro* and *in vivo* investigation

A. SALEH[1], T.A. EL-MASRY[2], W.A. NEGM[3], B. ALOTAIBI[1], M.E. ELHARTY[4], K.N. ALOTAIBI[5], E. ELEKHNAWY[6]

[1]Department of Pharmaceutical Sciences, College of Pharmacy, Princess Nourah Bint Abdulrahman University, Riyadh, Saudi Arabia
[2]Department of Pharmacology and Toxicology, Faculty of Pharmacy, Tanta University, Tanta, Egypt
[3]Department of Pharmacognosy, Faculty of Pharmacy, Tanta University, Tanta, Egypt
[4]Study Master in Pharmaceutical Science at the Institute of Research and Environmental Studies, El Sadat City, Egypt
[5]Health Services Directorate, Ministry of Defense, Riyadh, Saudi Arabia
[6]Pharmaceutical Microbiology Department, Faculty of Pharmacy, Tanta University, Tanta, Egypt

Abstract. – OBJECTIVE: It is highly required to find novel alternatives to the antibiotics currently used due to the increasing dissemination of antibiotic resistance among bacteria, especially enteric bacteria. The current study aimed to produce selenium nanoparticles (SeNPs) by *Euphorbia milii* Des Moul leaves extract (EME).

MATERIALS AND METHODS: The produced SeNPs were characterized using different techniques. After that, *in vitro* and *in vivo* antibacterial activity against *Salmonella typhimurium* was elucidated. Moreover, phytochemical identification and quantification of the chemical compositions of EME were performed using HPLC. The broth microdilution method determined the minimum inhibitory concentrations (MICs).

RESULTS: The MIC values of SeNPs ranged from 128 to 512 µg/mL. Additionally, the impact of SeNPs on membrane integrity and permeability was investigated. A marked decline in the membrane integrity and inner and outer membrane permeability was noticed in 50%, 46.15%, and 50% of the tested bacteria, respectively. Subsequently, a gastrointestinal tract infection model was used to study the *in vivo* antibacterial potential of SeNPs. Remarkably, treatment with SeNPs resulted in average-sized intestinal villi and colonic mucosa in the small intestine and caecum, respectively. In addition, it was revealed there was no inflammation or dysplasia in the studied tissues. SeNPs also enhanced the survival rate and significantly decreased the number of colony-forming units per gram tissues in the small intestine and caecum. Concerning the inflammatory markers, SeNPs significantly ($p < 0.05$) decreased interleukins (6 and 1β).

CONCLUSIONS: The biosynthesized SeNPs revealed antibacterial potential *in vivo* and *in vitro*; however, this finding should be elucidated clinically in the future.

Key Words:
GIT infection, HPLC, Membrane integrity, Membrane permeability, Proinflammatory cytokines.

Introduction

During the past decades, the concerns about bacterial infections have grown significantly owing to the significant threat to the healthcare system worldwide. Unfortunately, the world is going towards the post-antibiotic era due to disseminating misuse of antibiotics, which spread resistance to the current antibiotics[1].

Now, nanotechnology provides solutions for different medical problems because it employs materials with tiny dimensions (below 100 nm) and a high biological activity owing to their high ratios of surface to volume[2]. However, various nanomaterials are available, such as polymeric, metallic, and biomolecule-based nanomaterials. These nanomaterials have been widely studied in the current years to reveal their different biological activities[3].

However, the drawbacks of the chemical and physical nanoparticle synthesis methods on the

Corresponding Author: T.A. El-Masry, MD; e-mail: thanaa.elmasri@pharm.tanta.edu.eg

environment limited their use. Thus, it was essential to find environmentally friendly alternative methods of synthesis. Therefore, incorporating green synthesis methods, in which living organisms are used to produce nanomaterials, could be a promising solution[4].

Moreover, one of the largest genera of medicinal plants, *Euphorbia,* is found in tropical nations such as China and Pakistan; however, it is a member of the *Euphorbiaceae* family. Meanwhile, in the literature the phytochemistry of many species of *Euphorbia* has been identified a variety of secondary metabolites, such as diterpenes, β-sitosterol, *p*-hydroxybenzoic acid, flavones, and flavonol glucosides. Further, the *Euphorbia* genus of plants has been widely studied for its pharmacological activities, which include anticancer, antiviral, and antibacterial effects[5].

Due to the fast emergence of nanotechnology, which has had a major effect on materials science, biomedicine, environment, agriculture, and industry during the last few decades, there have been great advances in science and technology over the past few decades[6,7]. Metal nanoparticles such as silver (Ag), gold (Au), cerium (Ce), iron (Fe), and selenium (Se) have attained a unique position in the field of nanotechnology due to their tremendous potential for delivering drugs, proteins, genes, and siRNA. They are also potential candidates for use as chemotherapeutic and anti-inflammatory agents. Since selenium is a semi-solid metal discovered in 1817 by Jon Jacob Berzelius, selenium nanoparticles have been studied the most[8]. Selenium nanoparticles (SeNPs) exhibit less cytotoxicity than selenium molecules and have a variety of therapeutic and diagnostic applications, making them potential components for clinical and biological applications[9,10].

Salmonella Typhimurium is a Gram-negative bacterium that belongs to the *Enterobacteriaceae* family. This species is regarded as one of the most common reasons for food poisoning caused by food or water consumption contaminated with this pathogen. It results in gastroenteritis in humans and can infect many hosts. These pathogenic bacteria are acquiring resistance to many antibiotics[11]. Therefore, the current research aimed to utilize *Euphorbia milii* as a natural source for producing SeNPs. Subsequently, the characterization of the produced nanoparticles has been evaluated. Then, the *in vivo* and *in vitro* antibacterial activity of nanoparticles against *S. Typhimurium* isolates was examined.

Materials and Methods

Plant Materials, Chemicals, and Media

Euphorbia milii Des Moul leaves were gathered from a local garden in Gharbia Governorate in March 2021. Dr. Esraa Ammar, Plant Ecology department, Faculty of Science, Tanta University, confirmed the plant identification. A voucher specimen (PG-A-EM-W-16) was kept at the Plant Ecology Department. Leaf powder (250 g) was extracted three times with 70% methanol in water. Next, the aqueous extract was evaporated under reduced pressure to yield 18.96 g of *Euphorbia milii* extract residue (EME). All the utilized chemicals were purchased from Merck (Rahway, New Jersey, USA), while the culture medium was from Oxoid (Basingstoke, Hampshire, UK).

HPLC Analysis

High performance liquid chromatography (HPLC) analysis of the EME was performed according to Seliem et al[12] and Attallah et al[6].

Green Synthesis of SeNPs

For environmentally friendly SeNP synthesis, the previously reported method by Ramamurthy et al[13] was conducted. The EME is combined with a selenium precursor salt (sodium selenite solution, 1 mM) and heated at 50°C for 48 hours to produce nanoparticles. The nanoparticles are synthesized, then collected by centrifugation, washed with water several times, and dried before usage.

Characterization of the Synthesized SeNPs

The characterization was conducted by a JEOL JEM-2100 high-resolution transmission electron microscope (TEM, Akishima, Tokyo, Japan) at a 200-kV accelerating voltage. The air-dried powder form of the samples was ground with KBr pellets for Fourier transform infrared spectroscopy (FTIR) measurements (SHIMADZU, Kyoto, Nakagyo-ku, Japan). The diffuse reflectance mode of a Thermo Nicolet model 6700 spectrum instrument (Waltham, Massachusetts, USA) with a resolution of 4 cm^{-1} was used for analysis. Subsequently, 512 scans were recorded to get a satisfactory signal-to-noise ratio. The resulting peaks were plotted with wave number (cm^{-1}) on the Y axis and percent transmittance on the X axis. Using the Malvern Particle Size Analyzer MS2000 (Malvern, Worcestershire, UK), the dynamic light scattering (DLS) method was used to examine the size distribution of SeNPs[14,15].

In Vitro Antibacterial Potential

Bacteria

Twenty-six *Salmonella Typhimurium* clinical isolates from the department of microbiology and immunology at Tanta University, Tanta, Egypt, have been used.

Agar well diffusion assay

It was carried out as previously reported[16] on Muller-Hinton agar (MHA) plates. The bacterial suspensions were spread on the MHA surface using sterile cotton swabs. The wells were produced in the MHA plates. Subsequently, SeNPs (1000 µg/mL) were added to the wells with positive and negative controls. The MHA plates were incubated for 24 h at 37°C and inspected for the appearance of inhibition zones around the wells.

Minimum inhibitory concentrations (MICs)

The MIC values were detected as the minimum concentration of SeNPs, which can inhibit the growth of bacteria. The broth microdilution method was employed using microtiter 96-well plates[17]. However, the utilized concentrations of SeNPs had a range from 1 to 1024 µg/mL. Positive and negative controls were used; the plates were incubated for 24 h at 37°C.

Influence on the membrane integrity

As previously reported, the integrity of the membrane was elucidated by measuring the absorbance at 260 nm using a UV-Vis spectrophotometer (SHIMADZU, Nakagyo-ku, Kyoto, Japan)[18].

Influence on the membrane permeability

The impact of SeNPs on the inner and outer cell membrane permeability was investigated. Briefly, the inner membrane permeability was studied by tracking the discharge of β-galactosidase enzyme from inside the cell to the outside using O-nitrophenyl-β-galactopyranoside (ONPG) as a substrate for the enzyme. As a result of the enzyme's activity, O-nitrophenol (ONP) was formed; meanwhile, its quantity was measured at 420 nm by an ELISA reader (Sunrise Tecan, Seestrasse, Männedorf, Switzerland)[19]. The outer membrane permeability was investigated by adding the fluorescent agent 1-N-phenylnapthylamine (NPN)[19]. Using a fluorescence spectrophotometer (SHIMADZU, Nakagyo-ku, Kyoto, Japan), the fluorescence was determined at excitation and emission wavelengths of 340 and 420 nm, respectively.

In Vivo Antibacterial Activity

Animals

Forty adult Swiss albino mice, weighing 22-26 g, were obtained from the animal house of Cairo University, Egypt. Mice were given filtered water with a standard pellet at room temperature. The Committee of the Research Ethics of the Faculty of Pharmacy at Tanta University, Egypt, authorized the experimental procedures (code number was TP/RE/1/23P-004).

Experimental model

Mice were allocated into four groups as follows (n = 10 mice)[20]:

- Group I (normal control): they took the regular diet.
- Group II (*S. Typhimurium* group): they took *S. Typhimurium* (1×10^6 CFU/mL) orally[21].
- Group III (ciprofloxacin treated, 10 mg/kg): they took ciprofloxacin orally twice a day for three days. The first dose was 12 h after infection.
- Group IV (SeNPs treated, 10 mg/kg): they took SeNPs orally twice daily for three days. The first dose was 12 h after infection.

Animals were observed for two weeks, and their survival rate was calculated. At the end of the experiment, the remaining alive animals were anesthetized and euthanized; meanwhile, their small intestine and caecum were removed for the histological, immunohistochemical, and biochemical investigations. Besides, the burden was detected in the small intestine and caecum by determination of the number of colony-forming units (CFU/g)[22].

Histological evaluation

Small intestine and caecum samples were put in 10% formalin. After dehydration, they were placed in paraffin wax and spliced into thin sections. Further, sections were stained with hematoxylin and eosin (H&E)[23,24]. Photos were captured for the stained sections.

Immunohistochemical exploration

Polyclonal antibodies of the tumor necrosis factor-alpha (TNF-α) and nuclear factor kappa B (NF-κβ), purchased from Invitrogen (Carlsbad, CA, USA), were implemented in the immunohistochemical investigation. The immunostaining degrees were either negative, weak, moderate, or strong, as previously reported[7,25].

Biochemical studies

The proinflammatory biomarkers, including interleukin 6 and 1β (IL-6 and IL-1β), were evaluated in the small intestine and caecum using ELISA.

Statistical Analysis

The test results were revealed as mean ± standard deviation (SD) with n = 3. An ANOVA with a post hoc test (Tukey) was employed to assess the differences among the groups. A significant difference was considered if $p < 0.05$. The Kaplan-Meier survival curve was performed to assess the animals' survival in the experimental groups using Prism software version 8 (GraphPad, San Diego, CA, USA).

Results

Chemical Composition HPLC Analysis

The identification and quantification of the chemical composition of EME were performed using HPLC. Figure 1 represents the HPLC chromatogram for EME's identified flavonoids and phenolic compounds. The HPLC experiment allowed for the identification of 16 compounds. However, the abundant phenolic compound was chlorogenic acid (7.34 µg/mL), while the major identified flavonoid compound was naringenin (30.19 µg/mL), as shown in Table I.

Characterization of the Synthesized SeNPs

The color of the solution changed from pale yellow to red during the SeNPs synthesis process, signifying the reduction of SeNPs. Fourier transform infrared (FT-IR) analysis was utilized to evaluate the presence of functional groups at 400-4000 cm^{-1}, as shown in Figure 2. Transmission electron microscopy (TEM) was used to assess the morphology and size distribution of the biosynthesized SeNPs, as shown in Figure 3. The produced SeNPs had particle sizes less than 50 nm and spheroidal shapes. SeNPs were evenly scattered. The results of this study agree with previous findings[9,14]. Using zeta potential and dynamic light scattering (DLS) analysis (Figure 4), the stability and hydrodynamic size of synthesized SeNPs were evaluated. In addition, the zeta potential measures the surface charge of nanoparticles. Therefore, the nanoparticle size distribution was carried out at room temperature and under ideal circumstances.

In Vitro Antibacterial Activity

SeNPs revealed antibacterial activity against *S. Typhimurium* as there were inhibition zones around the wells in the agar diffusion assay. The MIC values were determined using the broth microdilution method, ranging from 128 to 512 µg/mL.

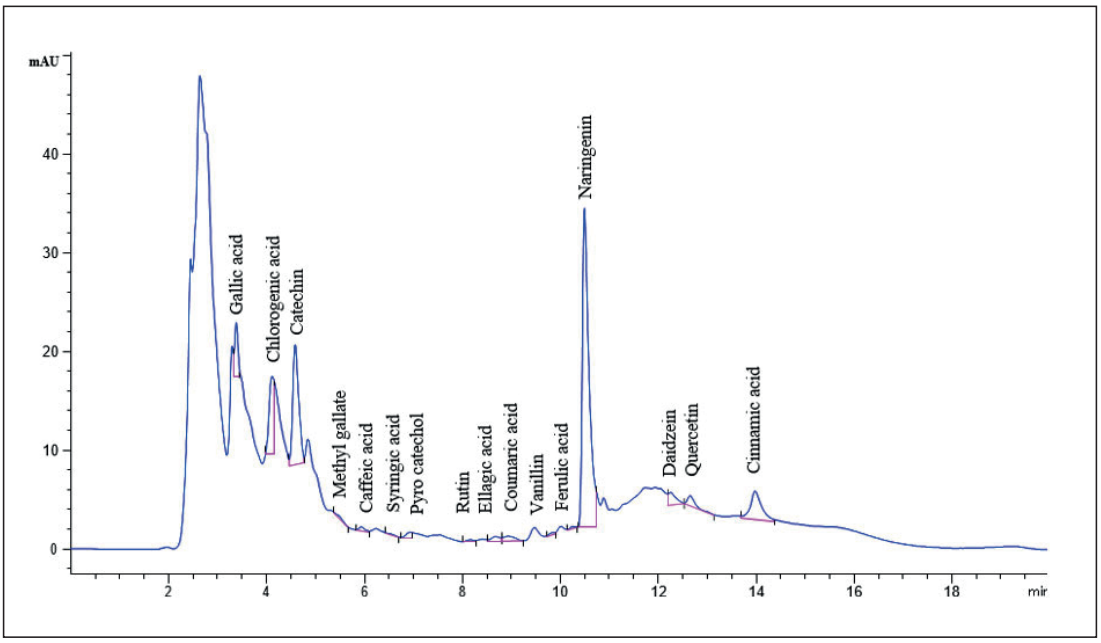

Figure 1. HPLC chromatogram for the identified compounds.

Table I. Phytochemical analysis of EME phenolic and flavonoid compounds using HPLC.

	RT (Min)	Area (mAU*s)	Conc. (µg/mL)	Identified compound
1	3.38	25.80	2.07	Gallic acid
2	4.11	52.09	7.34	Chlorogenic acid
3	4.59	102.95	26.79	Catechin
4	5.5	2.19	0.14	Methyl gallate
5	5.93	3.34	0.29	Caffeic acid
6	6.57	1.09	0.11	Syringic acid
7	6.94	4.24	0.56	Pyro catechol
8	8.16	1.71	0.23	Rutin
9	8.68	5.82	1.02	Ellagic acid
10	8.94	8.24	0.24	Coumaric acid
11	9.86	1.93	0.11	Vanillin
12	10.25	1.38	0.11	Ferulic acid
13	10.5	297.11	30.19	Naringenin
14	12.25	13.07	0.89	Daidzein
15	12.65	9.67	1.19	Quercetin
16	13.98	45.03	1.08	Cinnamic acid

Membrane Integrity

The impact of SeNPs on the integrity of the bacterial membranes was elucidated by detecting the release of the materials with absorption at 260 nm from the bacterial cells. The results exhibited a marked decrease in the membrane integrity in 50% of the tested bacteria (Figure 5).

Membrane Permeability

A marked increase in the permeability of the bacterial inner membrane was noticed after treatment with SeNPs in 46.15% of the isolates (Figure 6A). The outer membrane permeability increased considerably after treatment with SeNPs in 50% of the tested isolates (Figure 6B).

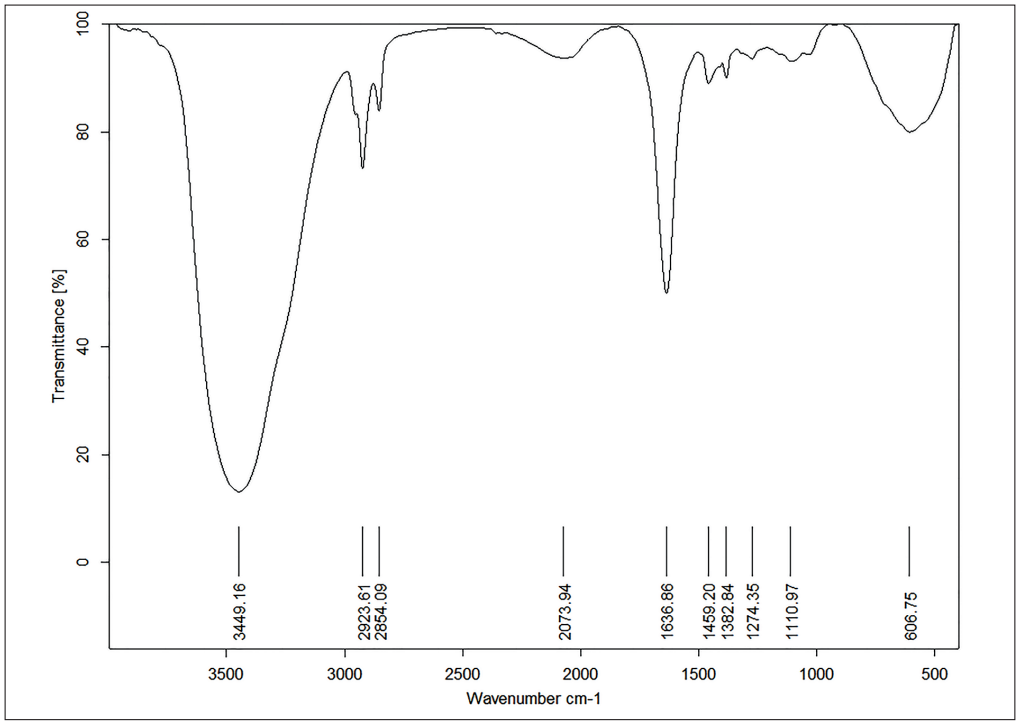

Figure 2. FTIR spectrum of synthesized SeNPs.

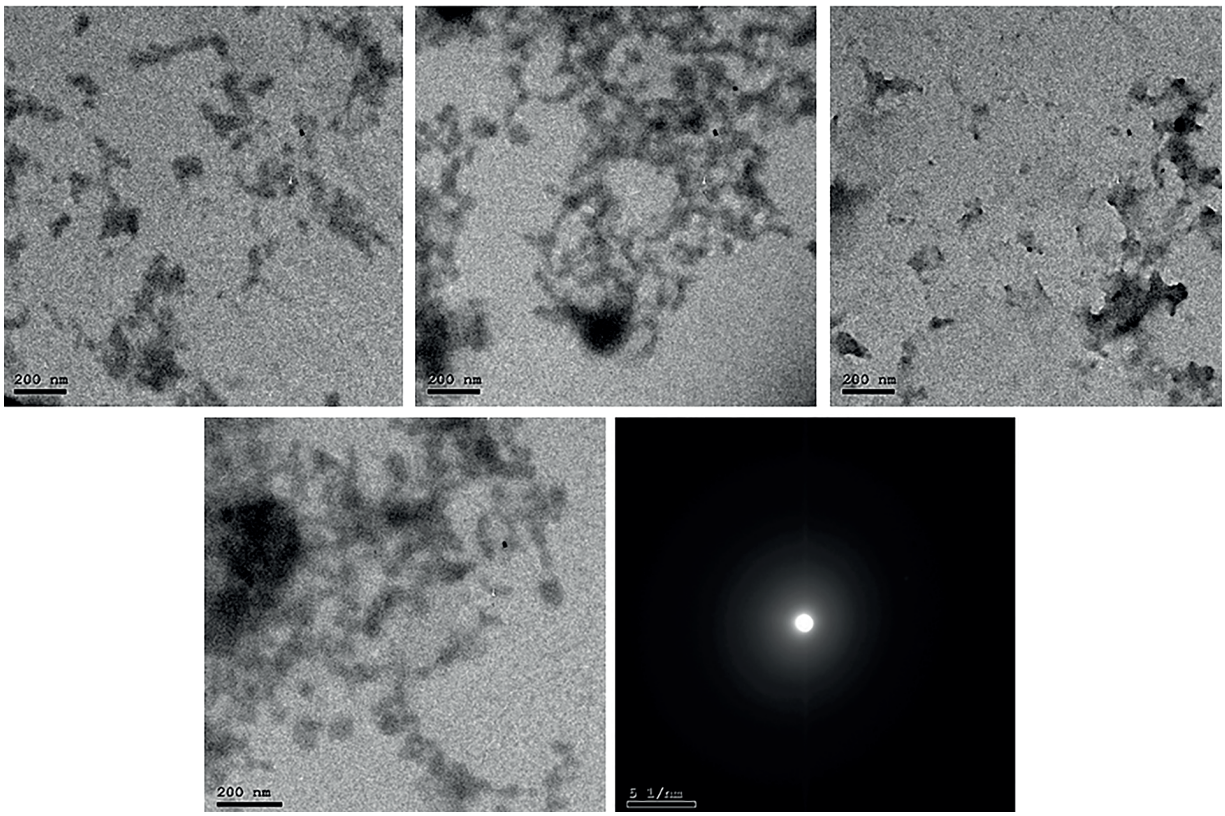

Figure 3. TEM images of the prepared SeNPs.

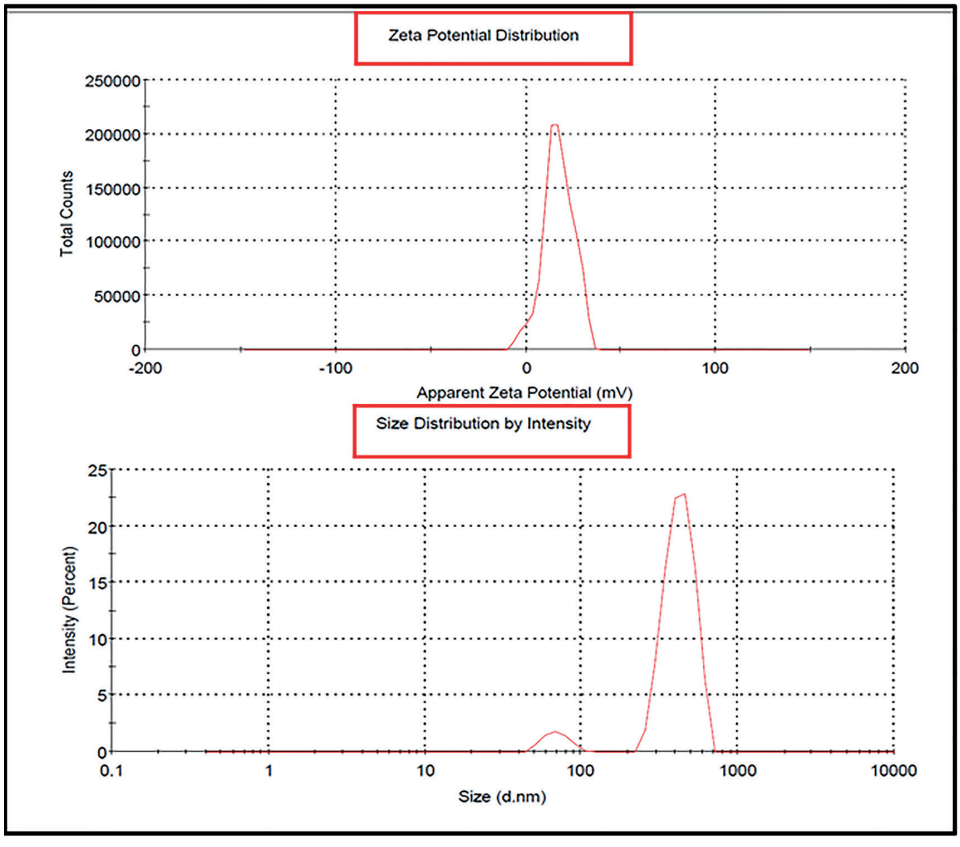

Figure 4. DLS diagram and zeta potential of synthesized SeNPs.

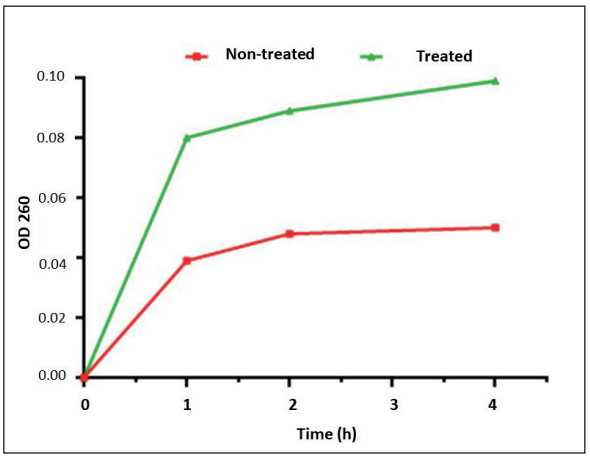

Figure 5. Linear charts reveal a representative example of increasing the discharge of the material absorbing at 260 nm after treatment with SeNPs, indicating their destructive effect on the membrane (i.e., they decrease the membrane integrity).

In Vivo Antibacterial Activity

Bacterial burden and survival are presented in Figure 7. SeNPs significantly declined the count of CFU/g tissues of the small intestine and caecum ($p < 0.05$).

Moreover, SeNPs improved the survival rate of the infected mice (Figure 8). Regarding group I, all mice remained alive. In group II, two mice died after six days, one after seven days, other two after eight days, and two after thirteen days. Concerning group III, only one mouse died after four days, and another one died after ten days. In group IV, two mice only passed after a week.

Histology

Hematoxylin and eosin (H&E) staining was used to assess the influence of SeNPs on the histological features of the small intestine and caecum, as revealed in Figure 9 and Figure 10.

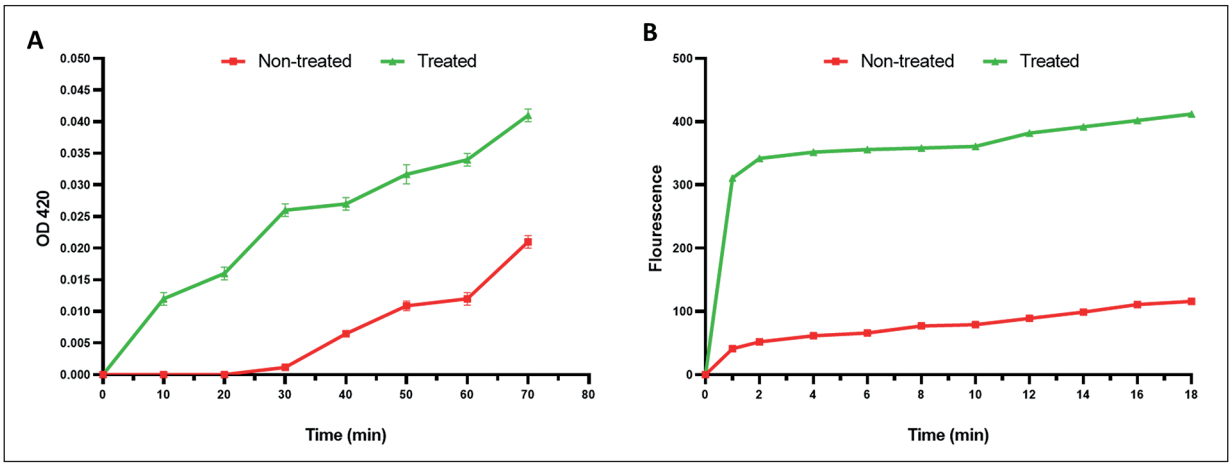

Figure 6. Linear charts display the impact of SeNPs on inner membrane permeability (**A**) and outer membrane permeability (**B**).

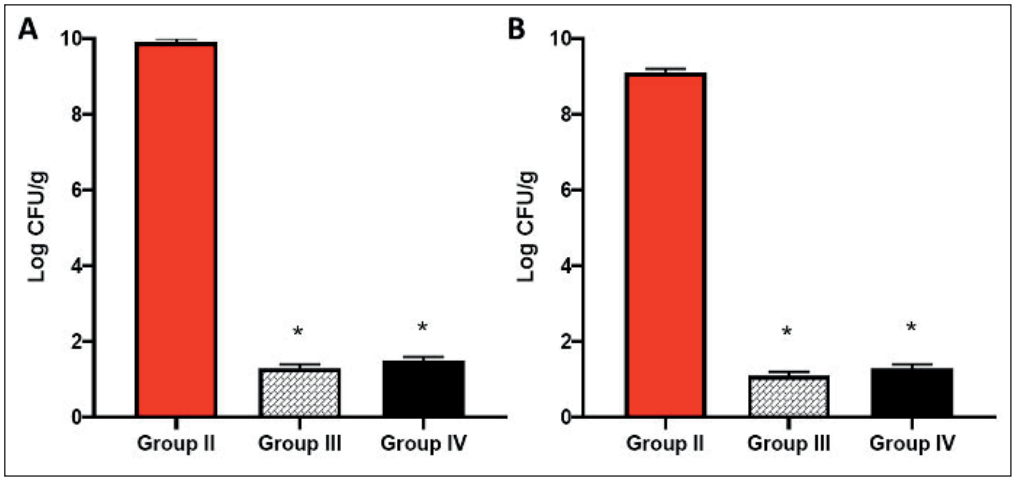

Figure 7. The count of CFU/mL. **A**, small intestine and caecum (**B**).

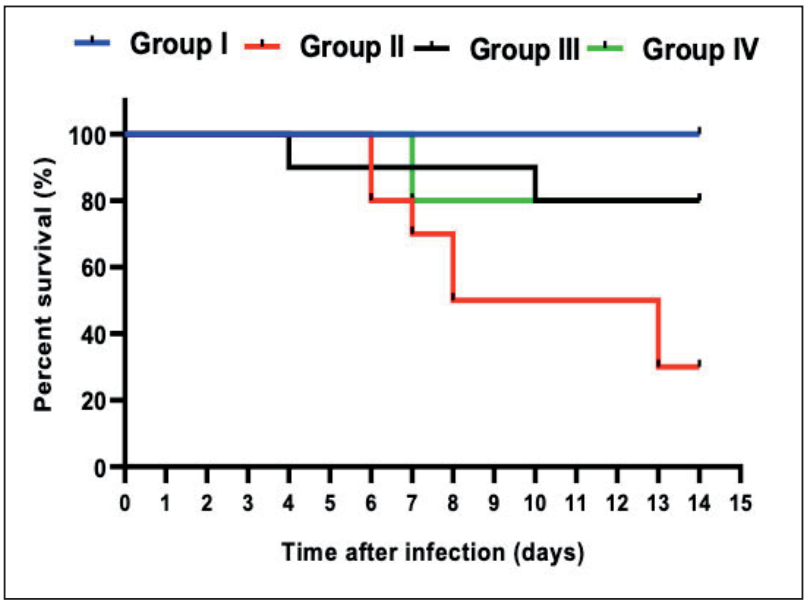

Figure 8. Survival curve of the different groups.

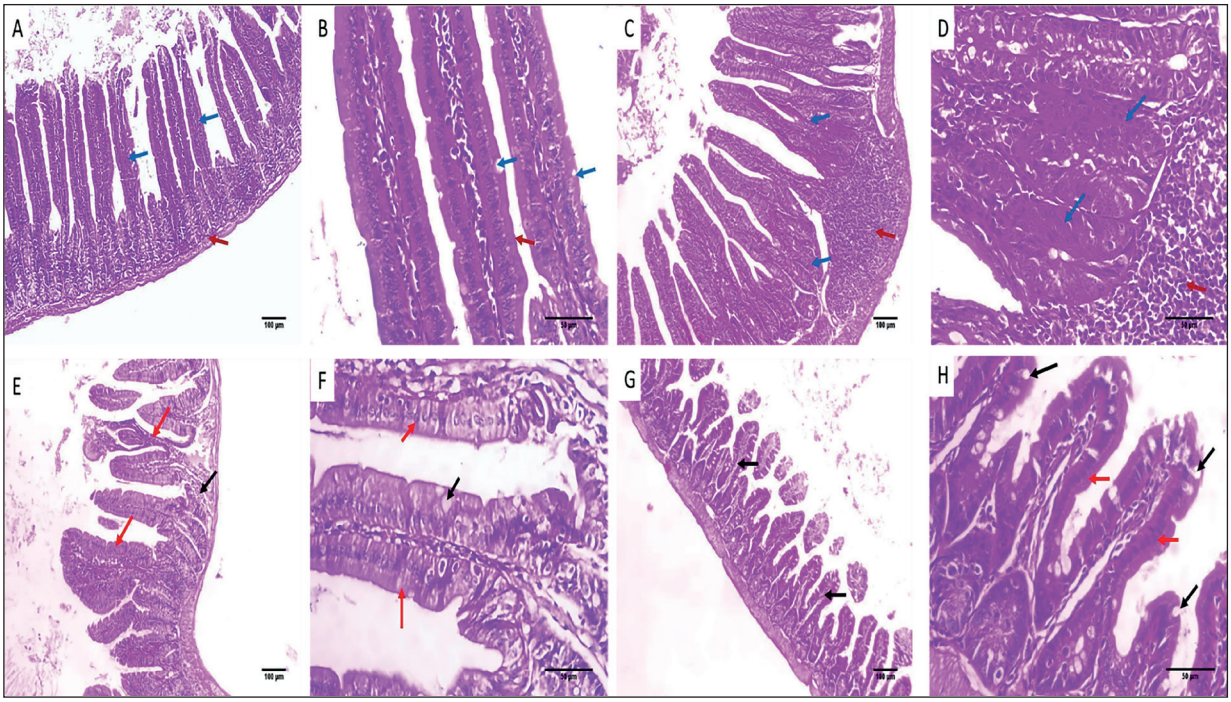

Figure 9. H&E stained sections of the small intestine. **A**, Group I exhibit average-sized intestinal villi (blue arrows) with underlying submucosa and serosa (red arrow) (×100). **B**, A higher magnification of group I exhibit villi (red arrow) lined with columnar cells with goblet cells (blue arrows) (×400). **C**, Group II reveals disrupted intestinal villi (blue arrows) with underlying chronic inflammation with infiltration of the inflammatory cells (red arrow) (×100). **D**, A higher magnification of group II exhibits disrupted intestinal villi with mild epithelial dysplasia (hyperchromasia with depletion of goblet cells, blue arrows) with underlying chronic inflammation manifested by infiltration of the inflammatory cells (red arrow) (×400). **E**, Group III exhibits a mild disrupted intestinal villus (red arrows) with focal chronic inflammation (black arrow) (×100). **F**, A higher magnification of group III exhibits average-sized intestinal villi (red arrows) with columnar cells lining and few goblet cells (black arrow) with no dysplasia and normal tissues (×400). **G**, Group IV reveals average-sized intestinal villi (black arrows) with no inflammation or dysplasia and normal tissues (×100). **H**, A higher magnification of group IV exhibits average-sized intestinal villi (red arrows) with columnar cells lining and many goblet cells (black arrows) with no dysplasia and normal tissues (×400).

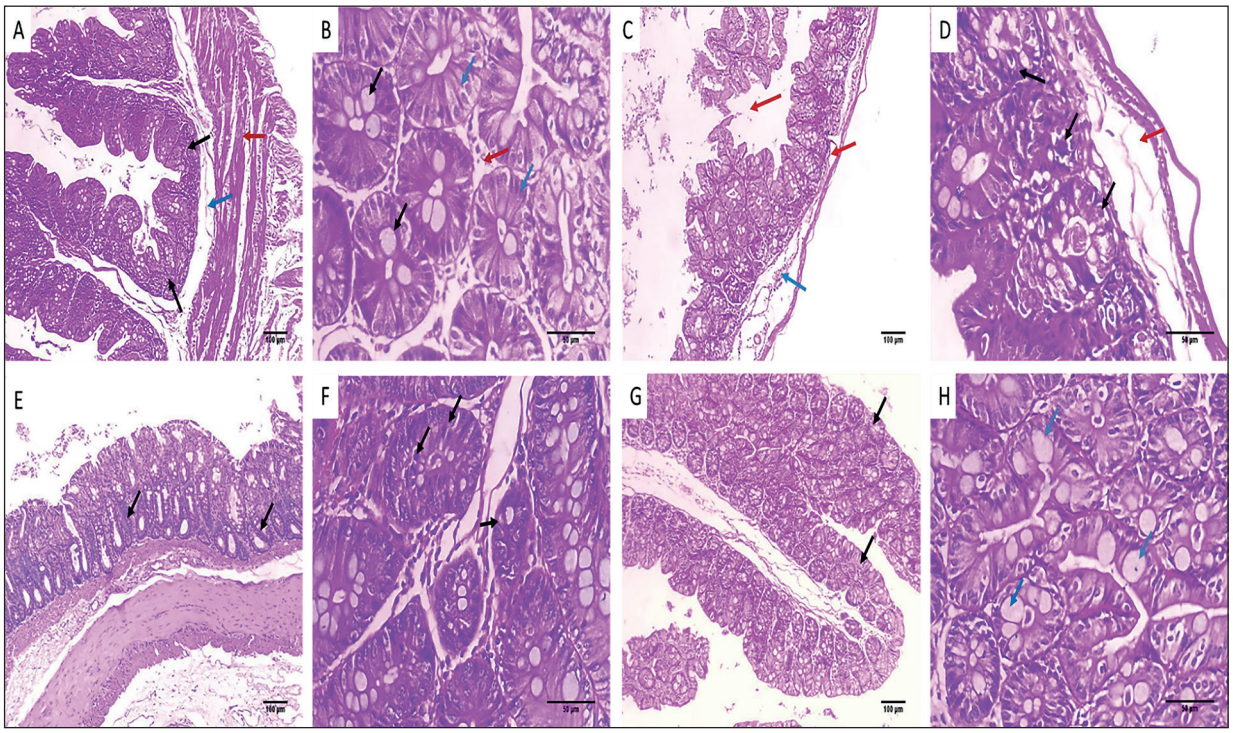

Figure 10. H&E stained sections of the caecum. **A**, Group I reveal average-sized colonic mucosa (black arrow) with underlying normal submucosa (blue arrow) and muscularis mucosae (red arrow) (×100). **B**, A higher magnification of group I exhibits normal colonic mucosal glands, average in size and shape, lined with columnar cells (blue arrows) and goblet cells (black arrows) separated by fibroblastic stroma (red arrow) (×400). **C**, Group II exhibits disrupted colonic mucosa and muscularis mucosae (red arrows) with underlying focal chronic inflammation with infiltration of the inflammatory cells (blue arrow) (×100). **D**, A higher magnification of group II exhibits disrupted colonic mucosa and muscularis mucosae (red arrow) with mild dysplasia (hyperchromasia with depletion of goblet cells, black arrows) (×400). **E**, Group III is exhibiting normal colonic mucosa with focal basal dysplasia (black arrows) (×100). **F**, A higher magnification of group III exhibits colonic glands with mild focal dysplasia (black arrows) with no inflammation (×400). **G**, Group IV is exhibiting a normal average-sized colonic mucosa (black arrows) with no inflammation or dysplasia (×100). **H**, A higher magnification of group IV exhibits average-sized colonic glands with many goblet cells (blue arrows) with no dysplasia (×400).

Immunohistochemistry

TNF-α and NF-κβ immunostained sections of the small intestine and caecum are revealed in Figures 11-14.

ELISA

The analysis showed that SeNPs significantly reduced ($p < 0.05$) the proinflammatory interleukins (IL-6 and IL-1β), as revealed in Table II.

Discussion

Misusing different antibiotics has led to the development and spread of bacterial resistance. In addition, a few newly discovered antibiotics cannot withstand the disseminating resistance to various antibiotics. Therefore, there is a need to reveal alternative approaches to treatment[26]. Here, the green synthesis approach was employed to synthesize SeNPs from EME. After the complete characterization of the formed nanoparticles, their antibacterial potential against *S. Typhimurium* isolates was elucidated. The SeNPs had MIC values of 128 to 512 µg/mL. Other researchers reported that SeNPs possessed antibacterial activity against Gram-negative bacteria like *Serratia marcescens*, *Alcaligenes faecalis*, and *Enterobacter cloacae*[14]. In addition, they revealed inhibitory potential against *Salmonella abony*, *Escherichia coli*, *Klebsiella pneumoniae*, and *Pseudomonas aeruginosa*[9].

Many antibacterial agents use the cell membranes of bacteria as their main target[27]. Herein, membrane integrity was studied before and after treatment with SeNPs; however, a marked decrease in membrane integrity was noticed in 50% of the tested bacteria. Membrane integrity defines the quality of the bacterial membrane.

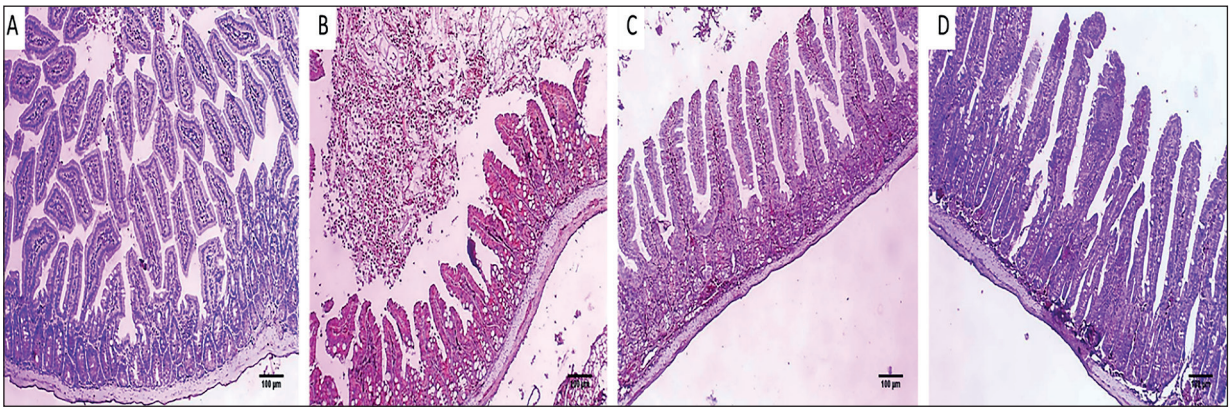

Figure 11. TNF-α immunostained sections of the small intestine. **A**, Group I is exhibiting a negative TNF-α expression (no positively immunostained cells, score 0) (×100). **B**, Group II is exhibiting a marked TNF-α expression (88% positively immunostained cells, score 4) (×100). **C**, Group III is exhibiting a moderate TNF-α expression (33% positively immunostained cells, score 2) (×100). **D**, Group IV exhibits a weak TNF-α expression (15% positively immunostained cells, score 1) (×100).

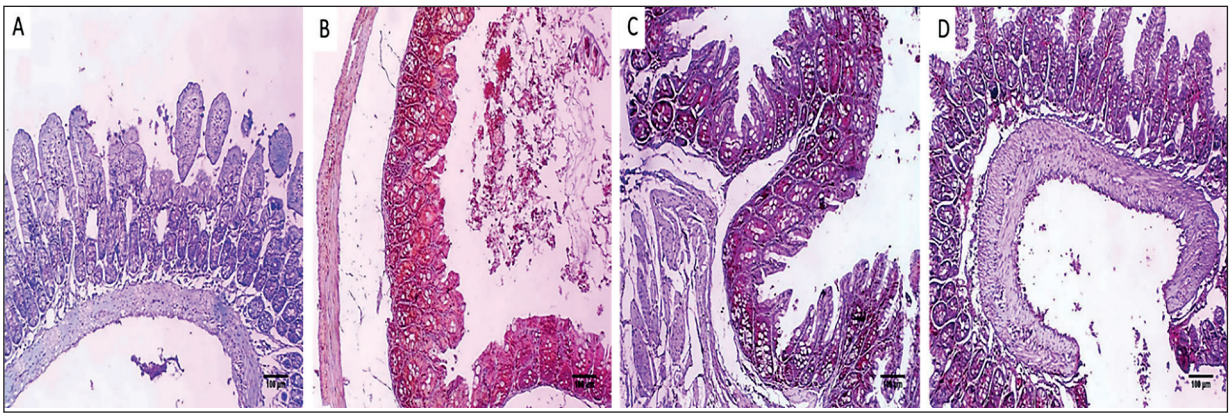

Figure 12. TNF-α immunostained sections of the caecum. **A**, Group I is exhibiting a negative TNF-α expression (no positively immunostained cells, score 0) (×100). **B**, Group II is exhibiting a marked TNF-α expression (90% positively immunostained cells, score 4) (×100). **C**, Group III is exhibiting a strong TNF-α expression (52% positively immunostained cells, score 3) (×100). **D**, Group IV exhibits a moderate TNF-α expression (26% positively immunostained cells, score 2) (×100).

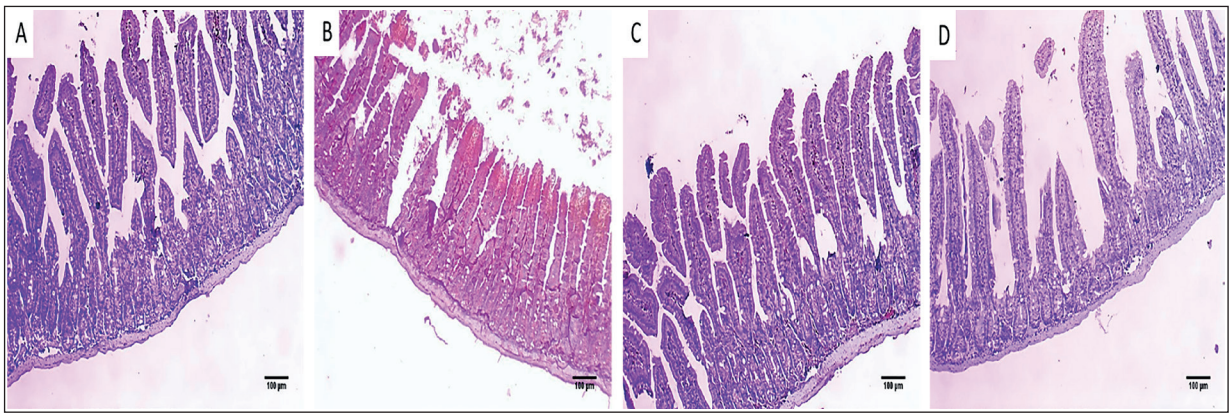

Figure 13. NF-κβ immunostained sections of the small intestine. **A**, Group I is exhibiting a negative NF-κβ expression (no positively immunostained cells, score 0) (×100). **B**, Group II is exhibiting a marked NF-κβ expression (93% positively immunostained cells, score 4) (×100). **C**, Group III is exhibiting a weak NF-κβ expression (12% positively immunostained cells, score 1) (×100). **D**, Group IV exhibits a negative NF-κβ expression (no positively immunostained cells, score 0) (×100).

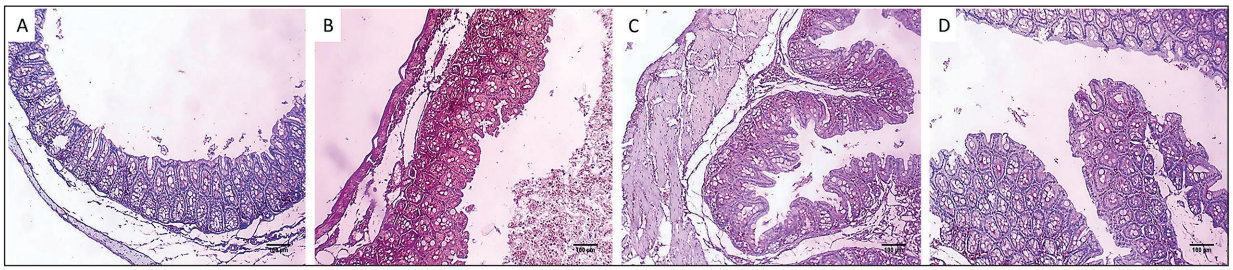

Figure 14. NF-κβ immunostained sections of the caecum. **A**, Group I is exhibiting a negative NF-κβ expression (no positively immunostained cells, score 0) (×100). **B**, Group II is exhibiting a marked NF-κβ expression (78% positively immunostained cells, score 4) (×100). **C**, Group III is exhibiting a moderate NF-κβ expression (30% positively immunostained cells, score 2) (×100). **D**, Group IV exhibits a weak NF-κβ expression (14% positively immunostained cells, score 1) (×100).

Table II. The proinflammatory interleukins (IL-6 and IL-1β) in different groups.

Groups	IL-6 (pg/mg tissues)		IL-1β (pg/mg tissues)	
	Small intestine	Caecum	Small intestine	Caecum
Group I	77.2 ± 1.2*	78.5 ± 6.5*	20.8 ± 4.5*	21.1 ± 2.1*
Group II	252 ± 2.3	239.2 ± 4.2	80.4 ± 5.7	89 ± 3.6
Group III	103.6 ± 3.3*	95.7 ± 2.3*	24.5 ± 5.4*	19.4 ± 2.2*
Group IV	110.8 ± 4.2*	103 ± 5.3*	29 ± 3.3*	26.6 ± 3.1*

*Indicates a significant difference ($p < 0.05$) compared to group II.

When the bacterial membrane is negatively affected and its integrity decreases, the release of nucleic acids (DNA and RNA) increases outside the cell[27]. Another essential characteristic of the bacterial membrane is its permeability. Gram-negative bacteria like *S. Typhimurium* possess two membranes: the outer and inner membranes. Here, the influence of SeNPs on the outer and inner membrane permeability was elucidated. Noticeably, SeNPs increased the inner and outer membrane permeability in 46.15% and 50% of the isolates, respectively. The membranes of the bacterial cell act as a vital compartment, which helps in the maintenance of cellular homeostasis and consequently conserves different physiological processes. Furthermore, they act as a barrier that preserves the bacterial cells[28]. Previous studies[29-31] have reported the influence of various nanoparticles, such as cerium oxide NPs[29], zinc oxide NPs[30], silver NPs[6], and titanium oxide NPs[31], on bacterial membrane permeability.

However, *S. Typhimurium* is one of the most common pathogenic bacteria that cause gastroenteritis; thus, a gastrointestinal tract *in vivo* model was conducted to elucidate the antibacterial activity of SeNPs. Furthermore, SeNPs exhibited promising *in vivo* antibacterial activity as they improved the small intestine and caecum histological findings. Treatment with SeNPs resulted in average-sized villi in the small intestine and average-sized colonic mucosa in the caecum with no inflammation or dysplasia.

Regarding the inflammation markers, the impact of treatment with SeNPs on different inflammation markers like TNF-α, IL-6, and IL-1β was elucidated. The results explored that the inflammation markers increased in the infected tissues to initiate the inflammatory process[22]. In the group treated with SeNPs, there is a remarkable decline in the proinflammatory interleukins (IL-6 and IL-1β) compared to the control group. Additionally, the TNF- α immunostaining decreased in the small intestine and caecum of the group treated with SeNPs. Regarding NF-κB, a

transcription factor essential for the inflammatory response[32], its immunostaining was declined in the SeNPs-treated group.

To our knowledge, this is the first study elucidating the *in vivo* (using an oral infection model in mice to simulate the real infection with this enteric pathogenic bacterium) and *in vitro* (by studying its effect on the membrane characters of the tested bacteria) antibacterial activity of the green synthesized SeNPs by EME against *S. Typhimurium*[32,33].

Conclusions

This study underlined the green synthesis of SeNPs by EME as a cheap, simple, and harmless method compared to physical or chemical processes. The SeNPs were characterized using different techniques, including UV, TEM, FTIR, DLS, and DRD. The antibacterial activity of SeNPs was elucidated *in vitro* and *in vivo*. SeNPs revealed a remarkable antibacterial action against *S. Typhimurium* clinical isolates. In addition, it affected membrane integrity and permeability. Concerning the *in vivo* effect, the SeNPs treated group exhibited a reduction in dysplasia and inflammation, as noticed in the histological, immunohistochemical, and ELISA studies. Conclusively, SeNPs could be efficient future candidates that can be elucidated for their effectiveness against other gastrointestinal tract infections.

Acknowledgements
This work was funded by the Deanship of Scientific Research at Princess Nourah bint Abdulrahman University, Riyadh, Saudi Arabia, through the Research Groups Program Grant no.(RGP-1440-0022)(2). The authors gratefully acknowledge the DSR technical and financial support.

Ethics Approval
The study was conducted according to the guidelines approved by the Research Ethics Committee of the Faculty of Pharmacy, Tanta University (approval code TP/RE/1/23p-004).

Availability of Data and Materials
The data presented in this study are available on request from the corresponding author.

Conflict of Interest
The authors declare no conflict of interest.

Authors' Contributions
A. Saleh, T. A. El-Masry: funding supervision, data curation, and formal analysis. W.A. Negm, B. Alotaibi, and E. Elekhnawy: conceptualization, investigation, writing, review, and editing. M. E. Elharty, and K. N. Alotaibi: methodology, and software. All authors have read and agreed to the published version of the manuscript.

References

1) Geoffrion LD, Hesabizadeh T, Medina-Cruz D, Kusper M, Taylor P, Vernet-Crua A, Chen J, Ajo A, Webster TJ, Guisbiers G. Naked selenium nanoparticles for antibacterial and anticancer treatments. ACS omega 2020; 5: 2660-2669.
2) Mabrouk M, Das DB, Salem ZA, Beherei HH. Nanomaterials for biomedical applications: Production, characterisations, recent trends and difficulties. Molecules 2021; 26: 1077-1083.
3) Jeevanandam J, Barhoum A, Chan YS, Dufresne A, Danquah MK. Review on nanoparticles and nanostructured materials: history, sources, toxicity and regulations. Beilstein j nanotechnol 2018; 9: 1050-1074.
4) Baig N, Kammakakam I, Falath W. Nanomaterials: A review of synthesis methods, properties, recent progress, and challenges. Mat Adv 2021; 2: 1821-1871.
5) Saleem H, Zengin G, Locatelli M. In vitro biological propensities and chemical profiling of Euphorbia milii Des Moul (Euphorbiaceae): A novel source for bioactive agents. Ind Crops Prod 2019; 130: 9-15.
6) Attallah NG, Elekhnawy E, Negm WA, Hussein IA, Mokhtar FA, Al-Fakhrany OM. In vivo and in vitro antimicrobial activity of biogenic silver nanoparticles against Staphylococcus aureus clinical isolates. Pharmaceuticals 2022; 15: 194-214.
7) Alherz FA, Negm WA, Elekhnawy E, El-Masry TA, Haggag EM, Alqahtani MJ, Hussein IA. Silver nanoparticles prepared using Encephalartos laurentianus De wild leaf extract have inhibitory activity against Candida albicans clinical isolates. JOF 2022; 8: 1005.
8) Nayak V, Singh KR, Singh AK, Singh RP. Potentialities of selenium nanoparticles in biomedical science. New J Chem 2021; 45: 2849-2878.
9) Filipović N, Ušjak D, Milenković MT, Zheng K, Liverani L, Boccaccini AR, Stevanović MM. Comparative study of the antimicrobial activity of selenium nanoparticles with different surface chemistry and structure. Fron Bioeng Biotechnol 2021; 8: 621-630.
10) Cui D, Liang T, Sun L, Meng L, Yang C, Wang L, Liang T, Li Q. Green synthesis of selenium nanoparticles with extract of hawthorn fruit in-

duced HepG2 cells apoptosis. Pharm Biol 2018; 56: 528-534.

11) Chlebicz A, Śliżewska K. Campylobacteriosis, salmonellosis, yersiniosis, and listeriosis as zoonotic foodborne diseases: a review. IJERPH 2018; 15: 863-880.

12) Seliem EM, Azab ME, Ismail RS, Nafeaa AA, Alotaibi BS, Negm WA. Green coffee bean extract normalize obesity-induced alterations of metabolic parameters in rats by upregulating adiponectin and GLUT4 levels and reducing RBP-4 and HOMA-IR. Life 2022; 12: 693-713.

13) Ramamurthy C, Sampath K, Arunkumar P, Kumar MS, Sujatha V, Premkumar K, Thirunavukkarasu C. Green synthesis and characterization of selenium nanoparticles and its augmented cytotoxicity with doxorubicin on cancer cells. Bioprocess Biosyst Eng 2013; 36: 1131-1139.

14) Hernández-Díaz JA, Garza-García JJ, León-Morales JM, Zamudio-Ojeda A, Arratia-Quijada J, Velázquez-Juárez G, López-Velázquez JC, García-Morales S. Antibacterial activity of biosynthesized selenium nanoparticles using extracts of Calendula officinalis against potentially clinical bacterial strains. Molecules 2021; 26: 5929-5942.

15) Sharma G, Sharma AR, Bhavesh R, Park J, Ganbold B, Nam JS, Lee SS. Biomolecule-mediated synthesis of selenium nanoparticles using dried Vitis vinifera (raisin) extract. Molecules 2014; 19: 2761-2770.

16) Attallah NG, Al-Fakhrany OM, Elekhnawy E, Hussein IA, Shaldam MA, Altwaijry N, Alqahtani MJ, Negm WA. Anti-biofilm and antibacterial activities of Cycas media R. Br secondary metabolites: In silico, in vitro, and in vivo approaches. Antibiotics 2022; 11: 993-1011.

17) Almukainzi M, El-Masry TA, Negm WA, Elekhnawy E, Saleh A, Sayed AE, Ahmed HM, Abdelkader DH. Co-delivery of gentiopicroside and thymoquinone using electrospun m-PEG/PVP nanofibers: In-vitro and in vivo studies for antibacterial wound dressing in diabetic rats. Inter J Pharm 2022; 625: 106-118.

18) Mohd Yusof H, Abdul Rahman NA, Mohamad R, Hasanah Zaidan U, Samsudin AA. Antibacterial potential of biosynthesized zinc oxide nanoparticles against poultry-associated foodborne pathogens: an in vitro study. Animals 2021; 11: 2093-2110.

19) Alotaibi B, Mokhtar FA, El-Masry TA, Elekhnawy E, Mostafa SA, Abdelkader DH, Elharty ME, Saleh A, Negm WA. Antimicrobial activity of Brassica rapa L. flowers extract on gastrointestinal tract infections and antiulcer potential against indomethacin-induced gastric ulcer in rats supported by metabolomics profiling. J Inflamm Res 2021; 14: 7411-1423.

20) Alandiyjany MN, Abdelaziz AS, Abdelfattah-Hassan A, Hegazy WA, Hassan AA, Elazab ST, Mohamed EA, El-Shetry ES, Saleh AA, ElSawy NA. Novel *in vivo* assessment of antimicrobial efficacy of ciprofloxacin loaded mesoporous silica nanoparticles against Salmonella typhimurium infection. Pharmaceuticals 2022; 15: 357-367.

21) Mudakavi RJ, Raichur AM, Chakravortty D. Lipid coated mesoporous silica nanoparticles as an oral delivery system for targeting and treatment of intravacuolar Salmonella infections. RSC advances 2014; 4: 61160-61166.

22) Abdelkader DH, Negm WA, Elekhnawy E, Eliwa D, Aldosari BN, Almurshedi AS. Zinc oxide nanoparticles as potential delivery carrier: Green synthesis by Aspergillus niger endophytic fungus, characterization, and in vitro/in vivo antibacterial activity. Pharmaceuticals 2022; 15: 1057-1065.

23) Abdelkader DH, Elekhnawy E, Negm WA, El-Masry TA, Almukainzi M, Zayed A, Ulber R. Insight into fucoidan-based PEGylated PLGA nanoparticles encapsulating methyl anthranilic acid: in vitro evaluation and in vivo anti-inflammatory study. Mar Drugs 2022; 20: 694-710.

24) Al-Kuraishy HM, Al-Gareeb AI, Albogami SM, Jean-Marc S, Nadwa EH, Hafiz AA, Negm WA, Kamal M, Al-Jouboury M, Elekhnawy E. Potential therapeutic benefits of metformin alone and in combination with sitagliptin in the management of type 2 diabetes patients with COVID-19. Pharmaceuticals 2022; 15: 1361-1373.

25) Miotto A, Lins TA, Montero E, Oshima C, Alonso LG, Perfeito J. Immunohistochemical analysis of the COX-2 marker in acute pulmonary injury in rats. IJAE 2009; 114: 193-199.

26) Murugaiyan J, Kumar PA, Rao GS, Iskandar K, Hawser S, Hays JP, Mohsen Y, Adukkadukkam S, Awuah WA, Jose RAM. Progress in alternative strategies to combat antimicrobial resistance: Focus on antibiotics. Antibiotics 2022; 11: 200-215.

27) Chitemerere TA, Mukanganyama S. Evaluation of cell membrane integrity as a potential antimicrobial target for plant products. BMC complement altern med 2014; 14: 1-8.

28) Halder S, Yadav KK, Sarkar R, Mukherjee S, Saha P, Haldar S, Karmakar S, Sen T. Alteration of zeta potential and membrane permeability in bacteria: a study with cationic agents. SpringerPlus 2015; 4: 1-14.

29) Bellio P, Luzi C, Mancini A, Cracchiolo S, Passacantando M, Di Pietro L, Perilli M, Amicosante G, Santucci S, Celenza G. Cerium oxide nanoparticles as potential antibiotic adjuvant. Effects of CeO2 nanoparticles on bacterial outer membrane permeability. Biochim Biophy Acta Biomemb 2018; 1860: 2428-2435.

30) Patra P, Roy S, Sarkar S, Mitra S, Pradhan S, Debnath N, Goswami A. Damage of lipopolysaccharides in outer cell membrane and production of ROS-mediated stress within bacteria makes nano zinc oxide a bactericidal agent. App Nanosci 2015; 5: 857-866.

31) Ahmed B, Ameen F, Rizvi A, Ali K, Sonbol H, Zaidi A, Khan MS, Musarrat J. Destruction of cell topography, morphology, membrane, inhibition of respiration, biofilm formation, and bioactive molecule production by nanoparticles of Ag, ZnO, CuO, TiO2, and Al2O3 toward beneficial soil bacteria. ACS omega 2020; 5: 7861-7876.

32) Taniguchi K, Karin M. NF-κB, inflammation, immunity and cancer: coming of age. Nat Rev Immunol 2018; 18: 309-324.